Heterometal Dependence of Electron Distributions and Redox Potentials in Clusters with Cubane-Type $[MFe_3S_4]^z$ Cores

Wei Cen, Sonny C. Lee,[1a] Jiguo Li, Frederick M. MacDonnell,[1b] and R. H. Holm*

Contribution from the Department of Chemistry, Harvard University, Cambridge, Massachusetts 02138

Received May 7, 1993®

Abstract: The self-assembly systems $[MS_4]^{3-}/FeCl_2/NaSEt$ (M = V, Nb) in acetonitrile afford the clusters $[V_2Fe_6S_8(SEt)_9]^{3-}$, $[Nb_2Fe_6S_8(SEt)_9]^{3-}$, and $[Nb_2Fe_6S_8(SEt)_9]^{5-}$, which were isolated as Et_4N^+ salts. These clusters have the triply-bridged double cubane stereochemistry $[(MFe_3S_4(SEt)_3)_2(\mu\text{-}SEt)_3]^{3-}$, as demonstrated for the M = V cluster by X-ray diffraction. The compound $(Et_4N)_3[V_2Fe_6S_8(SEt)_9]$ crystallizes in hexagonal point group $P6_3/m$ with a = 17.223(3) Å, c = 16.212(3) Å, and Z = 2. The cluster anion has imposed D_{3h} symmetry; the individual clusters are separated by a V···V distance of 3.601 Å. These clusters, together with others previously reported, form a set $[M_2Fe_6S_8(SEt)_9]^{3-}$ whose members (M = V, Nb, Mo, W, Re) possess the same charge, identical ligands, and essentialy congruent structures with only small metric differences. This condition permits the examination of changes in heterometal on cluster properties. Redox potentials for the reversible couples $[M_2Fe_6S_8(SEt)_9]^{3-/4-}$ and $[M_2Fe_6S_8(SEt)_9]^{4-/5-}$ decrease in the order M = V > Nb > Mo > W > Re and parallel the trend in ^{57}Fe isomer shifts, M = V < Nb ≈ Mo < W ≈ Re. Reductions become more difficult as the ferrous character of the core increases. Redox reactions are accompanied by changes in electron density that largely occur in Fe_3S_4 cluster portions. The concept of cuboidal Fe_3S_4 as a cluster ligand is considered in terms of isomer shifts of heterometal clusters. The shifts of the majority of such clusters are close to those protein-bound $[Fe_3S_4]^{0,1-}$, providing an apparent definition of oxidation states. Isotropic shifts of ligands at iron sites provide a convenient indicator of the ground spin state of the clusters. Cubane-type MFe_3S_4 clusters are of renewed interest in view of the occurrence of the cuboidal cluster fragment $MoFe_3S_3$ in the cofactor of nitrogenase. The possible relationship of these results to the FeMo-cofactor and the FeV-cofactor of nitrogenase is noted. If the cofactor of vanadium-containing nitrogenase has an analogous structure, properties that derive from the heterometal cuboidal fragment may be influenced by vanadium vs molybdenum in a manner similar to that for the cubane-type clusters.

Introduction

Elsewhere we have introduced the concept of the Fe_3S_4 cuboidal fragment **1** as a quasirigid cluster ligand[2,3] in the formation and stabilization of the MFe_3S_4 heterometal cubane-type clusters whose core unit **2** is shown in Figure 1. Thus, linear $[Fe_3S_4]^+$ clusters rearrange under reducing conditions to **1** which captures reductant metal M to form **2**,[3-7] protein-bound clusters $[Fe_3S_4]^{0,-}$ bind exogenous metal ions to generate **2**,[3,8-11] and the cluster self-assembly systems $[MS_4]^z/NaSR/FeCl_2$[2,3] afford clusters containing **2**.[2,3,12-17] The products in the latter systems are always double-cubane clusters with one or more bridge structures. Two types of bridges have been cleaved to yield single cubanes.[15] The most frequently assembled double cubane is the tris(μ_2-thiolato) cluster $[M_2Fe_6S_8(SR)_9]^{z-}$ (**3**, Figure 1), which is also among the first heterometal cubane-type clusters to have been prepared.[12,13,15,16] Their structures have been verified repeatedly by X-ray diffraction. The indicated core oxidation states of **3** are produced directly by synthesis or by redox reactions of isolated clusters.

In earlier work, we have synthesized clusters **3** with M = Mo,[12-15] W,[13] and Re[2,17] in self-assembly systems. Christou and Garner[16] have also obtained by similar means several M = Mo and W double cubanes of this type.[18] Unlike other heterometal cubanes known at the time (1987), a *single* cubane, $[VFe_3S_4Cl_3(solv)_3]^-$, was prepared in an assembly system containing the obligatory tetrathiometalate but lacking thiolate.[19,20] Since then, the tetrathiometalates $[NbS_4]^{3-}$ and $[TaS_4]^{3-}$, previously unknown in soluble form, have been prepared in this laboratory.[21] As shown here, these species and $[VS_4]^{3-}$ are precursors in assembly systems leading to additional double

® Abstract published in *Advance ACS Abstracts*, September 1, 1993.

(1) (a) National Science Foundation Predoctoral Fellow, 1987–1990. (b) Damon Runyon-Walter Winchell Foundation Postdoctoral Fellow, 1992–1994.

(2) Ciurli, S.; Holm, R. H. *Inorg. Chem.* **1991**, *30*, 743.

(3) Holm, R. H. *Adv. Inorg. Chem.* **1992**, *38*, 1. This article is a comprehensive treatment of MFe_3S_4 clusters.

(4) (a) Ciurli, S.; Yu, S.-B.; Holm, R. H.; Srivastava, K. K. P.; Münck, E. *J. Am. Chem. Soc.* **1990**, *112*, 8169. (b) Ciurli, S.; Ross, P. K.; Scott, M. J.; Yu, S.-B. *J. Am. Chem. Soc.* **1992**, *114*, 5415.

(5) Zhou, J.; Scott, M. J.; Hu, Z.; Peng, G.; Münck, E.; Holm, R. H. *J. Am. Chem. Soc.* **1992**, *112*, 10843.

(6) Roth, E. K. H.; Greneche, J. M.; Jordanov, J. *J. Chem. Soc., Chem. Commun.* **1991**, 105.

(7) Coucouvanis, D.; Al-Ahmad, S. A.; Salifoglou, A.; Papaefthymiou, V.; Kostikas, A.; Simopoulos, A. *J. Am. Chem. Soc.* **1992**, *114*, 2472.

(8) Moura, I.; Moura, J. J. G.; Münck, E.; Papaefthymiou, V.; LeGall, J. *J. Am. Chem. Soc.* **1986**, *108*, 349.

(9) Surerus, K. K.; Münck, E.; Moura, I.; Moura, J. J. G.; LeGall, J. *J. Am. Chem. Soc.* **1987**, *109*, 3805.

(10) (a) Conover, R. C.; Park, J.-B.; Adams, M. W. M.; Johnson, M. K. *J. Am. Chem. Soc.* **1990**, *112*, 4562. (b) Srivastava, K. K. P.; Surerus, K. K.; Conover, R. C.; Johnson, M. K.; Park, J.-B.; Adams, M. W. W.; Münck, E. *Inorg. Chem.* **1993**, *32*, 927.

(11) (a) Butt, J. N.; Armstrong, F. A.; Breton, J.; George, S. J.; Thomson, A. J.; Hatchikian, E. C. *J. Am. Chem. Soc.* **1991**, *113*, 6643. (b) Butt, J. N.; Sucheta, A.; Armstrong, F. A.; Breton, J.; Thomson, A. J.; Hatchikian, E. C. *J. Am. Chem. Soc.* **1991**, *113*, 8948.

(12) Wolff, T. E.; Berg, J. M.; Hodgson, K. O.; Frankel, R. B.; Holm, R. H. *J. Am. Chem. Soc.* **1979**, *101*, 4140.

(13) Wolff, T. E.; Power, P. P.; Frankel, R. B.; Holm, R. H. *J. Am. Chem. Soc.* **1980**, *102*, 4694.

(14) Christou, G.; Mascharak, P. K.; Armstrong, W. H.; Papaefthymiou, G. C.; Frankel, R. B.; Holm, R. M. *J. Am. Chem. Soc.* **1982**, *104*, 2820.

(15) Holm, R. H.; Simhon, E. D. In *Molybdenum Enzymes*; Spiro, T. G., Ed.; Wiley-Interscience: New York, 1985; Chapter 2.

(16) Christou, G.; Garner, C. D. *J. Chem. Soc., Dalton Trans.* **1980**, 2354.

(17) (a) Ciurli, S.; Carney, M. J.; Holm, R. H.; Papaefthymiou, G. C. *Inorg. Chem.* **1989**, *28*, 2696. (b) Ciurli, S.; Carrié, M.; Holm, R. H. *Inorg. Chem.* **1990**, *29*, 3493.

(18) Note that the corresponding selenido double cubanes $[M_2Fe_6Se_8(SEt)_9]^{3-}$ (M = Mo, W) have recently been prepared: Greaney, M. A.; Coyle, C. L.; Pilato, R. S.; Stiefel, E. I. *Inorg. Chim. Acta* **1991**, *189*, 81.

(19) $[VFe_2S_4Cl_4]^{3-}$ + $FeCl_2$ in DMF: (a) Kovacs, J. A.; Holm, R. H. *Inorg. Chem.* **1987**, *26*, 702, 711. (b) See also: Ciurli, S.; Holm, R. H. *Inorg. Chem.* **1989**, *28*, 1655.

0002-7863/93/1515-9515$04.00/0

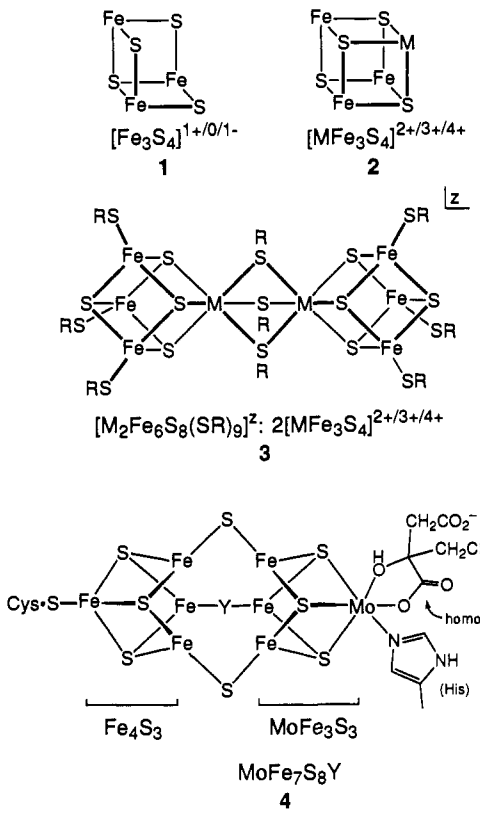

Figure 1. Structural formulas of the cuboidal Fe_3S_4 (**1**) and cubane-type MFe_3S_4 (**2**) cluster cores, the double-cubane cluster $[M_2Fe_6S_8(SEt)_9]^z$ (**3**), and the Kim–Rees FeMo-cofactor structure (**4**). When the latter is in the protein, the unique Fe atom is coordinated to a cysteinate sulfur and the Mo atom to bidentate homocitrate and an imidazole group of a histidine residue.[23]

cubanes **3**. These findings, together with the results of preceding work, now afford an expanded set of double-cubane clusters. Members of the set manifest the properties of constant terminal and bridging ligation, equal overall charge, and nearly invariant metric features in structures of fixed stereochemistry. Consequently, the response of properties such as redox potentials and cluster charge distribution to heterometal variation in the set $[M_2Fe_6S_8(SR)_9]^{3-}$ can now be examined meaningfully in a comparative sense.

In the bioinorganic context, clusters containing the core **2** still provide the best synthetic models for the immediate environment of molybdenum and vanadium atoms in the cofactors of their respective nitrogenases.[22] This matter has been documented at some length elsewhere.[3,15] The crystallographically based Kim–Rees structure **4** of the FeMo-cofactor,[23] which is depicted in Figure 1, confirms this resemblance. With the existence of two cofactors containing different metals, the property dependence of cubane or cuboidal clusters on the identity of heterometal assumes plausible significance. The first examination of this matter, utilizing the set of double cubanes **3**, is presented here.

(20) The only assembly systems shown to afford MFe_3S_4 single cubanes in the presence of anionic sulfur ligands are those containing $[MS_4]^{2-}/FeCl_2/R_2NCS_2^-$, which yield $[MFe_3S_4(R_2NCS_2)_5]^{0,-}$ (M = Mo, W): (a) Liu, Q.-T.; Huang, L.-R.; Kang, B.-S.; Liu, C.-W.; Wang, L.-L.; Lu, J. *Acta Chim. Sinica* **1986**, *2*, 107. (b) Lei, X.; Huang, Z.; Hong, M.; Liu, Q.; Liu, H. *Jiegou Huaxue (J. Struct. Chem.)* **1989**, *8*, 152. (c) Liu, Q.; Huang, L.; Liu, H.; Lei, X.; Wu, D.; Kang, B.; Lu, J. *Inorg. Chem.* **1990**, *29*, 4131.

(21) (a) Lee, S. C.; Holm, R. H. *J. Am. Chem. Soc.* **1990**, *112*, 9654. (b) Lee, S. C.; Li, J.; Mitchell, J. C.; Holm, R. H. *Inorg. Chem.* **1992**, *31*, 4333.

(22) Burgess, B. K. *Chem. Rev.* **1990**, *90*, 1377.

(23) (a) Kim, J.; Rees, D. C. *Science* **1992**, *257*, 1677; *Nature* **1992**, *360*, 553. (b) Chan, M. K.; Kim, J.; Rees, D. C. *Science* **1993**, *260*, 792. See also: (c) Bolin, J. T.; Ronco, A. E.; Morgan, T. V.; Mortenson, L. E. *Proc. Natl. Acad. Sci. U.S.A.* **1993**, *90*, 1078.

Experimental Section

Preparation of Compounds. All operations were performed in a pure dinitrogen atmosphere. Solvents were dried by standard methods and were distilled before use. The compounds $(Et_4N)_2[Fe(SEt)_4]$,[24] $(Pr_4N)[Fe(SEt)_4]$,[25] $(Me_3NCH_2Ph)_2[Fe_2S_2(SEt)_4]$,[24] $(Bu_4N)_2[Fe_4S_4(SEt)_4]$,[24] and $(Et_4N)_3[Fe_4S_4(S\mathit{t}Bu)_4]$,[26] used to investigate the correlation of isomer shifts and iron oxidation states, were prepared by published methods. The double-cubane cluster compounds $(Et_4N)_3[M_2Fe_6S_8(SEt)_9]$ (M = Mo,[12,16] Re[17b]) were obtained by literature procedures.

$(Et_4N)_3[V_2Fe_6S_8(SEt)_9]$. $(NH_4)_3[VS_4]$[27] (1.16 g, 4.98 mmol) and Et_4NCl (1.24 g, 7.49 mmol) were added to 150 mL of acetonitrile. The mixture was stirred vigorously and 1.90 g (15.0 mmol) of anhydrous $FeCl_2$ and then 3.00 g (35.7 mmol) of NaSEt was added. The deep brown mixture was stirred overnight and then filtered through a fine frit. Ether (80 mL) was diffused into the deep yellow-brown filtrate maintained at 5 °C for 5 days. Black hexagonal crystals were collected and washed twice with 1:1 acetonitrile:ether and then with ether to afford 2.90 g (71%) of product. Absorption spectrum (acetonitrile): λ_{max} (ϵ_M) 276 (49 500), 358 (36 800), 432 (sh, 34 100) nm. ^1H NMR (CD_3CN): δ 13.28 ($FeSCH_2$), 5.82 (V_2SCH_2), 3.15 ($FeSCH_2CH_3$), 2.60 ($V_2SCH_2CH_3$). Anal. Calcd for $C_{42}H_{105}Fe_6N_3S_{17}V_2$: C, 30.86; H, 6.49; Fe, 20.50; N, 2.57; S, 33.34; V, 6.23. Found: C, 31.05; H, 6.65; Fe, 20.41; N, 2.53; S, 33.18; V, 6.20.

$(Et_4N)_3[W_2Fe_6S_8(SEt)_9]$. This procedure is a modification of a literature preparation[16] that in our hands has given inconsistent results. To 80 mL of acetonitrile was added 0.761 g (6.00 mmol) of anhydrous $FeCl_2$, 1.01 g (12.0 mmol) of NaSEt, and 0.497 g (3.00 mmol) of Et_4NCl. The reaction mixture was stirred vigorously for 10 min and 0.701 g (200 mmol) of $(NH_4)_2[WS_4]$ was added, causing a slow color change from yellow-green to deep brown. The mixture was stirred overnight and filtered. Slow diffusion of ether into the filtrate gave large prism-like crystals. These were collected and washed as in the previous preparation to afford 0.412 g (22% of product) as black crystals, which were pure by an ^1H NMR criterion.[16] ^1H NMR spectrum (CD_3CN): δ 54.3 ($FeSCH_2$), 12.5 (W_2SCH_2), 4.59 ($FeSCH_2CH_3$), 1.07 ($W_2SCH_2CH_3$).

$(Et_4N)_3[Nb_2Fe_6S_8(SEt)_9]$. (a) Direct Synthesis. To a slurry of 63 mg (1.21 mmol) of LiOEt in 9 mL of acetonitrile was added 0.46 mL (2.18 mmol) of $(Me_3Si)_2S$. The reaction mixture was stirred until a clear solution formed; a solution of 175 mg (0.550 mmol) of $Nb(OEt)_5$ in 9 mL of ether was introduced. The mixture was stirred for 1 h, giving a white precipitate and an orange solution. Addition of 1.0 mL (6.6 mmol) of freshly distilled *N,N,N',N'*-tetramethylethylenediamine caused the precipitate to dissolve. This solution, which contains $[NbS_4]^{3-}$,[21] was diluted with 50 mL of acetonitrile and treated consecutively with 136 mg (0.825 mmol) of Et_4NCl, 209 mg (1.65 mmol) of anhydrous $FeCl_2$, and 330 mg (3.93 mmol) of NaSEt. A golden brown color quickly developed. The reaction mixture was stirred overnight and filtered through a fine frit. Analysis of a small aliquot of the filtrate by ^1H NMR indicated the formation of the desired cluster and $[Fe_4S_4(SEt)_4]^{2-}$ in a 2:1 ratio. The filtrate was concentrated in vacuo to a volume of *ca.* 15 mL. Ether (100 mL) was introduced by diffusion at 5 °C over 2 days, resulting in the separation of solid material as a brown powder and black needle-like crystals. The mixture was agitated such that the powder was removed with the mother liquor by cannula. The remaining solid was washed with copious quantities of ether to afford the product as 156 mg (33%) of black crystals. Absorption spectrum (acetonitrile): λ_{max} (ϵ_M) 246 (127 000), 353 (40 1000), 392 (sh, 38 000) nm. ^1H NMR (CD_3CN): δ 16.48 ($FeSCH_2$), 4.15 (Nb_2SCH_2), 2.56 ($FeSCH_2CH_3$), 2.50 ($V_2SCH_2CH_3$). Anal. Calcd for $C_{42}H_{105}Fe_6N_3Nb_2S_{17}$: C, 29.35; H, 6.16; Fe, 19.50; N, 2.45; Nb, 10.81; S, 31.74. Found: C, 30.43; H, 6.04; Fe, 18.82; N, 2.53; Nb, 11.35; S, 30.62. A single crystal of this compound is isomorphous with its vanadium analogue: hexagonal, a = 17.22(1) Å, c = 16.38(1) Å, space group $P6_3/m$, V = 4297(4) Å^3, Z = 2.

(b) Iodine Oxidation. To a solution of 5.00 g (2.53 mmol) of $(Et_4N)_5[Nb_2Fe_6S_8(SEt)_9]$ (vide infra) in 200 mL of acetonitrile, a solution of 0.321 g (1.26 mmol) of iodine in 50 mL of acetonitrile was added dropwise with stirring over 5 min. A gradual color change from yellow-brown to golden-brown ensued and a small quantity of black precipitate was formed. After addition was complete, the reaction mixture was stirred

(24) Hagen, K. S.; Watson, A. D.; Holm, R. H. *J. Am. Chem. Soc.* **1983**, *105*, 3905.

(25) Maelia, L. E.; Millar, M.; Koch, S. A. *Inorg. Chem.* **1992**, *31*, 4594.

(26) Hagen, K. S.; Watson, A. D.; Holm, R. H. *Inorg. Chem.* **1984**, *23*, 2984.

(27) Do, Y.; Simhon, E. D.; Holm, R. H. *Inorg. Chem.* **1985**, *24*, 4635.

Table I. Crystallographic Data[a] for $(Et_4N)_3[V_2Fe_6S_8(SEt)_9]$ (1)

formula	$C_{42}H_{105}Fe_6N_3S_{17}V_2$
formula wt	1634.29
cryst system	hexagonal
space group	$P6_3/m$ (no. 176)
Z	2
a, Å	17.223(3)
c, Å	16.212(3)
V, Å^3	4165(1)
ρ_{calc}, g/cm^3	1.30
T, K	173
μ, mm^{-1}	1.68
R^b (R_w^c), %	8.55 (6.15)

[a] All data were collected with graphite monochromatized Mo-Kα radiation (λ = 0.71069 Å) using ω-scans. [b] $R = \sum||F_o| - |F_c||/\sum|F_o|$. [c] $R_w = \{\sum[w(|F_o| - |F_c|)^2/\sum(w|F_o|^2)\}^{1/2}$, with the weighting scheme provided by a 3-term Chebyshev polynomial: Carruthers, J. R.; Watkin, D. J. *Acta Crystallogr.* **1979**, *A35*, 698.

for 30 min and then filtered through a medium glass frit, and the filtrate was filtered again through a very fine glass frit. The filtrate was concentrated to 100 mL and ether was introduced by diffusion over the period of about 1 week. The solid was collected by filtration and washed with ether to afford 1.35 g (31%) of product as black bar-like crystals. This product was identical in all respects to that obtained by method a.

$(Et_4N)_5[Nb_2Fe_6S_8(SEt)_9]$. To 60 mL of acetonitrile was added 320 mg (4.70 mmol) of sodium ethoxide followed by 1.30 mL (6.18 mmol) of $(Me_3Si)_2S$. The mixture was stirred until a clear solution formed. A solution of 500 mg (1.57 mmol) of $Nb(OEt)_5$ in 40 mL of acetonitrile was added and stirring was continued for 2 h. At this point, the reaction mixture consisted of an orange solution and a white solid. The latter was centrifuged from the solution, washed with ether, and dried in vacuo to a constant weight (to remove acetonitrile), affording 118 mg (0.409 mmol) of solid formulated as $Na_3[NbS_4]$. This freshly prepared material was suspended in 100 mL of acetonitrile, to which was added consecutively 580 mg (3.50 mmol) of Et_4NCl, 380 mg (3.00 mmol) of $FeCl_2$, and 590 mg (7.02 mmol) of NaSEt. The mixture was stirred for 2 days and filtered through a fine glass frit. Diffusion of ether into the filtrate at 5 °C over a week afforded black crystals and a light yellow powder. The solution and yellow solid were removed by cannula while the mixture was gently agitated. The black solid was washed thoroughly with ether, collected by filtration, and dried in vacuo to afford 181 mg (12%, based on $Nb(OEt)_5$) of black crystalline product. (This procedure can be scaled up by *ca.* 10-fold.) Absorption spectrum (acetonitrile): λ_{max} (ϵ_M) 242 (sh, 149 000), 398 (sh, 50 700) nm. Anal. Calcd for $C_{58}H_{145}Fe_6Nb_2S_{17}$: C, 35.21; H, 7.39; N, 3.54; Fe, 16.93; Nb, 9.39; S, 27.55. Found: C, 35.25; H, 7.54; N, 3.56; Fe, 16.86; Nb, 9.16; S, 27.41.

Collection and Reduction of X-ray Data. A black hexagonal crystal of $(Et_4N)_3[V_2Fe_6S_8(SEt)_9]$ was mounted as described previously.[21b] Diffraction data were collected with use of graphite-monochromatized Mo Kα radiation on a Siemens R3m/v four-circle automated diffractometer equipped with a Siemens LT-2 cryostat operating at 173 K. Following preliminary indexing, refined unit cell parameters were obtained by least-squares fits of 28 machine-centered reflections ($25° \le 2\theta \le 28°$). Data sets were processed and corrected for Lorentz and polarization effects with a locally modified version of XDISK (SHELXTL program suite, Siemens XRD Corp., Madison, WI); empirical absorption corrections (PSICOR) were applied with use of azimuthal Ψ-scan data. The intensities of three check reflections were monitored every 97 reflections with no significant decay observed over the course of data collection. Crystal parameters are provided in Table I.

Solution and Refinement of the Structure. The initial structure solution was obtained by direct methods (XS from SHELXTL). Axial photographs and intensities of symmetry-equivalent reflections indicated $6/m$ Laue symmetry, with systematic absences further narrowing the choice of space group to $P6_3$ (no. 173) or $P6_3/m$ (no. 176), with simple E statistics suggesting a centrosymmetric cell. The asymmetric unit consists of one-sixth of the anion and one-half of a cation. The positions of V, Fe, and S atoms were furnished by direct methods in $P6_3/m$; the choice of the proper space group was confirmed by successful refinement to convergence. Atoms not initially located by direct methods were found by successive Fourier or difference Fourier maps with intervening cycles of full-matrix least-squares refinement (CRYSTALS, with graphical interface provided by XP from SHELXTL). The methyl group (C(22)) of the bridging thiolate was symmetrically disordered across a mirror plane and was refined with an occupancy of 0.5. The ethyl groups of the terminal thiolate suffered from extreme disorder; each carbon atom was treated as being distributed between two sites, with occupancy factors refined and summed to unity and thermal parameters refined independently. Despite all efforts, chemically reasonable distances and angles could not be derived from these positions. All non-hydrogen atoms were treated anisotropically, with the exception of the disordered ethyl group of the terminal thiolate, which was refined isotropically. In the final stages of refinement, hydrogen atoms of the cation were placed at calculated positions 0.96 Å from, and with isotropic thermal parameters 1.2× those of, the parent carbon atoms. Final R factors are given in Table I.[28]

Table II. Redox Potentials[a] of $[M_2Fe_6S_8(SEt)_9]^{3-}$ in Acetonitrile Solution at 298 K

	V vs SCE			V vs SCE	
M	$E_p(3-/4-)$	$E_p(4-/5-)$	M	$E_p(3-/4-)$	$E_p(4-/5-)$
V	−0.99	−1.16	Mo	−1.26	−1.44
Nb	−1.00	−1.18	W	−1.38	−1.53
Ta	−1.05	−1.23	Re	−1.40	−1.64

[a] Peak potentials from differential pulse voltammetry: Pt working electrode, *ca.* 2 mM cluster, 0.1 M $(Bu_4N)PF_6$ supporting electrolyte.

Other Physical Measurements. All measurements were performed under anaerobic conditions. Spectrophotometric and ^{1}H NMR measurements were made with conventional equipment. Electrochemical measurements were carried out with a PAR Model 263 potentiostat/galvanostat; data were analyzed with use of PARC ECHEM software. Potentials are referenced to a SCE; other details are given in Table II. Magnetic measurements were performed with a Quantum Design SQUID magnetometer. Mössbauer spectra were collected on a modified Ranger MS-1500 instrument equipped with an external VT-1200L velocity transducer and a PA-1200 krypton proportional counter (Ranger Scientific, Burleson, TX). The source was ^{57}Co (25 mCi) diffused into a rhodium matrix. Spectra were collected in the constant velocity mode with a symmetric triangular velocity waveform. The spectrometer was equipped with a Janis Model 8DT superVaritemp dewar fitted with mylar windows. Freshly powdered samples were loaded in Delrin sample cups. The data were analyzed with use of WMOSS software (Web Research Co., Edina, MN). Isomer shifts are referenced to Fe metal at 298 K.

Results and Discussion

Cluster Synthesis. The self-assembly approach afforded the desired triply thiolato-bridged double cubanes $[M_2Fe_6S_8(SEt)_9]^{3-}$ containing the $[VFe_3S_4]^{3+}$ and $[NbFe_3S_4]^{3+}$ cores. Thus, reaction system 1 in acetonitrile (M^I = NH_4^+, Li^+, Na^+), stoichiometric except for excess NaSEt, produced the product cluster salts in 71% (M = V) and 33% (M = Nb) purified yields as isomorphous black hexagonal crystals. In the M = Nb system, $[NbS_4]^{3-}$ was generated in situ by a previous procedure;[21] the yield is based on the $Nb(OEt)_5$ precursor. The doubly reduced niobium cluster $[Nb_2Fe_6S_8(SEt)_9]^{5-}$ was formed by the apparent stoichiometry of reaction 2. In this preparation, $Na_3[NbS_4]$ was isolated prior to treatment with the other reactants. Based on the quantity of this compound, the reaction system contained reducing equivalents ($FeCl_2$, NaSEt) in excess of those required for reaction 2. These

$$2M^I_3[MS_4] + 6FeCl_2 + 9NaSEt + 3Et_4NCl \rightarrow (Et_4N)_3[M_2Fe_6S_8(SEt)_9] + 9NaCl + 6M^ICl \quad (1)$$

$$2Na_3[NbS_4] + 6FeCl_2 + 11NaSEt + 5Et_4NCl \rightarrow (Et_4N)_5[Nb_2Fe_6S_8(SEt)_9] + 17NaCl + EtSSEt \quad (2)$$

promote the formation of the reduced cluster, isolated in 12% yield based on $Nb(OEt)_5$ but 44% based on $Na_3[NbS_4]$. By means of iodine oxidation, $[Nb_2Fe_6S_8(SEt)_9]^{5-}$ provides a second route to $[Nb_2Fe_6S_8(SEt)_9]^{3-}$ (31% yield).

Although not pursued at length, attempts to prepare clusters containing the $TaFe_3S_4$ core in analogous assembly systems

(28) See the paragraph at the end of this article concerning supplementary material available.

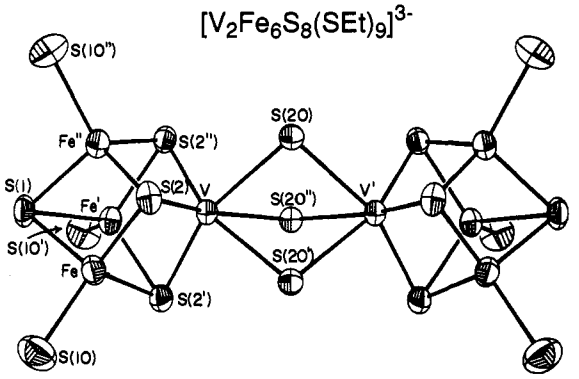

Figure 2. Structure of $[V_2Fe_6S_8(SEt)_9]^{3-}$ as its Et_4N^+ salt, showing the atom labeling scheme and 50% thermal ellipsoids; ethyl groups are omitted. Primed and unprimed atoms are symmetry related.

Table III. Selected Interatomic Distances (Å) and Angles (deg) for $[V_2Fe_6S_8(SEt)_9]^{3-}$

V–V′	3.601(3)	Fe–Fe′	2.687(1)
V–S(20)	2.520(1)	Fe–S(2)	2.244(1)
V–Fe	2.752(1)	Fe–S(1)	2.257(2)
V–S(2)	2.316(1)	Fe–S(10)	2.231(2)
V–S(20)–V′	91.20(7)	S(1)–Fe–S(2)	104.18(5)
S(20)–V–S(20′)	74.59(5)	S(1)–Fe–S(2′)	104.13(5)
S(2)–V–S(2′)	101.69(5)	S(2)–Fe–S(2′)	106.37(6)
S(2″)–V–S(20)	91.74(5)		
S(2)–V–S(20)	88.86(4)	S(2)–Fe–S(10)	115.38(6)
S(2′)–V–S(20)	160.73(6)	S(2′)–Fe–S(10)	116.11(6)
		S(1)–Fe–S(10)	109.46(7)
Fe–V–Fe′	58.45(3)		
Fe–Fe–Fe	60.00	Fe–S(1)–Fe′	73.04(6)
V–Fe–Fe′	60.78(2)	Fe–S(2)–Fe′	73.59(5)
V–S(2)–Fe	73.26(5)		
V–S(2)–Fe″	74.23(5)		

containing $[TaS_4]^{3-}$ gave inconsistent results. However, on several occasions very small quantities of a black crystalline solid as the Et_4N^+ salt were isolated whose cyclic voltammetry and ^1H NMR spectrum are entirely characteristic of the double cubane structure **3** (vide infra). The redox-active cluster is assigned as $[Ta_2Fe_6S_8(SEt)_9]^{3-}$; its potentials have been entered in Table II.

Structure of $[V_2Fe_6S_8(SEt)_9]^{3-}$. This cluster as its Et_4N^+ salt crystallizes in hexagonal space group $P6_3/m$ and is isomorphous with $(Et_4N)_3[M_2Fe_6S_8(SEt)_9]$ (M = Mo,[29a] W,[29b] Re[17b]) and $(Et_3NCH_2Ph)_3[Mo_2Fe_6S_8(SEt)_9]$.[12] The structure is set out in Figure 2 and selected metric parameters are listed in Table III. It is immediately apparent that the cluster possesses structure **3**. In this crystal, the cluster has an imposed C_3 axis on which are located atoms S(1,1′) and V,V′ and a perpendicular mirror plane containing atoms S(20,20′,20″), corresponding to molecular D_{3h} symmetry. In addition to the present cluster, the structures of five other double cubane trianions have been reported: $[Mo_2Fe_6S_8(SEt)_9]^{3-}$,[12,29a] $[Mo_2Fe_6S_8(SPh)_9]^{3-}$,[29c] $[Mo_2Fe_6S_8(SEt)_3(SCH_2CH_2OH)_6]^{3-}$,[30] $[W_2Fe_6S_8(SEt)_9]^{3-}$,[29b] and $[Re_2Fe_6S_8(SEt)_9]^{3-}$.[17b] Also, we have established that $(Et_4N)_3[Nb_2Fe_6S_8(SEt)_9]$ is isomorphous and isostructural with its vanadium counterpart.

The core structure of $[V_2Fe_6S_8(SEt)_9]^{3-}$ is congruent and virtually isometric with those of $[M_2Fe_6S_8(SEt)_9]^{3-}$ (M = Mo, Re), where sufficient data have been reported to allow accurate overall structural comparisons. The differences are those to be expected on the basis of variations among Shannon radii of M(III,IV) heterometals.[31] For example, in the M = V/Mo comparison bonded distances and angles differ by less than 0.05 Å and 2.0°, respectively. The largest systematic differences in the structures are the (nonbonded) M···M separations which increase in the order Re (3.543(3) Å) < V (3.601(3) Å) < Mo (3.64–3.67 Å) ≈ W (3.674(3) Å). Inasmuch as the structures of the Mo and Re clusters have been described in some detail, a corresponding discussion of $[V_2Fe_6S_8(SEt)_9]^{3-}$ is unnecessary.

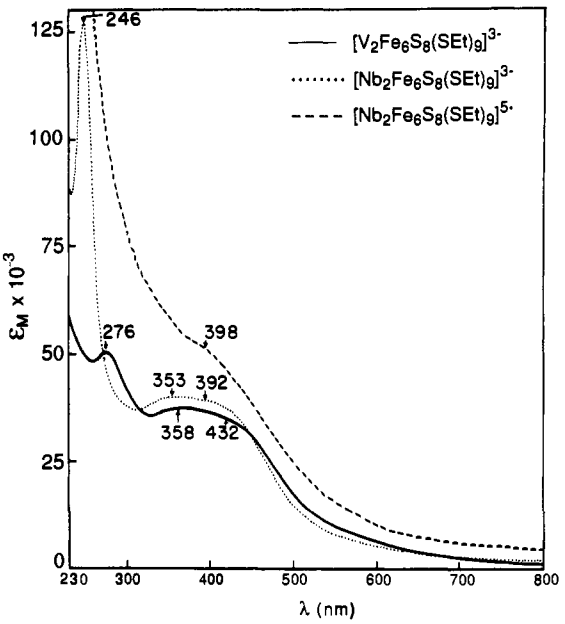

Figure 3. Absorption spectra of $[V_2Fe_6S_8(SEt)_9]^{3-}$, $[Nb_2Fe_6S_8(SEt)_9]^{3-}$, and $[Nb_2Fe_6S_8(SEt)_9]^{5-}$ in acetonitrile solution; band maxima are indicated.

The absorption spectra of $[V_2Fe_6S_8(SEt)_9]^{3-}$ and $[Nb_2Fe_6S_8(SEt)_9]^{3-}$, shown in Figure 3, are similar and are dominated by several strong bands in the 350–450-nm region; in this sense they resemble the spectra of other type **3** and related clusters.[12,13,32-34] These bands have been assigned as $RS^- \rightarrow$ core charge transfer transitions. Consistent with this description is the apparent blue shift of the two broad visible features of the $[Nb_2Fe_6S_8(SEt)_9]^{3-}$ spectrum (*ca.* 353, 392 nm) relative to the related bands in the $[V_2Fe_6S_8(SEt)_9]^{3-}$ spectrum (*ca.* 358, 432 nm). Evidently, the higher optical electronegativity of Nb vs V is reflected in the energies of the core frontier orbitals. The spectrum of $[Nb_2Fe_6S_8(SEt)_9]^{5-}$ is nearly featureless. The ^1H NMR spectrum of $[V_2Fe_6S_8(SEt)_9]^{3-}$, presented in Figure 4, exhibits small isotropic contributions to the chemical shifts (vide infra) and is entirely consistent with the solid-state structure. The spectrum of $[Nb_2Fe_6S_8(SEt)_9]^{3-}$ (not shown) is similarly consistent but with larger isotropic shifts. Terminal and bridging methylene signals integrate in a 2:1 ratio, further differentiating these clusters from the related $[M_2Fe_6S_9(SEt)_8]^{3-}$ (M = Mo, W) whose clusters are bridged by one sulfide and two ethanethiolate groups.[12,13]

With the availability of two additional examples of the double-cubane cluster $[M_2Fe_6S_8(SEt)_9]^{3-}$, we have at our disposal five clusters **3** with M = V, Nb, Mo, W, and Re which have identical charges and essentially congruent structures with only small metric differences. These species constitute the best available set of

(29) (a) Acott, S. R.; Christou, G.; Garner, C. D.; King, T. J.; Mabbs, F. E.; Miller, R. M. *Inorg. Chim. Acta* **1979**, *35*, L337. (b) Christou, G.; Garner, C. D.; Miller, R. M.; King, T. J. *J. Inorg. Biochem.* **1979**, *11*, 349. (c) Christou, G.; Garner, C. D.; Mabbs, F. E.; King, T. J. *J. Chem. Soc., Chem. Commun.* **1978**, 740.

(30) (a) Christou, G.; Garner, C. D.; Mabbs, F. E.; Drew, M. G. B. *J. Chem. Soc., Chem. Commun.* **1979**, 91. This cluster was originally formulated as $[Mo_2Fe_6S_8(SCH_2CH_2OH)_9]^{3-}$ but was later revised: (b) Palermo, R. E.; Power, P. P.; Holm, R. H *Inorg. Chem.* **1982**, *31*, 173.

(31) The maximum difference in octahedral radii within the set is 0.11 Å: Shannon, R. D. *Acta Crystallogr.* **1976**, *A32*, 751. Note that the structure of the M = V cluster was determined at 173 K and those of the other clusters at room temperature.

(32) Holm, R. H. *Chem. Soc. Rev.* **1981**, *10*, 485.

(33) Armstrong, W. H.; Mascharak, P. K.; Holm, R. H. *J. Am. Chem. Soc.* **1982**, *104*, 4373.

(34) Mascharak, P. K.; Armstrong, W. H.; Mizobe, Y.; Holm, R. H. *J. Am. Chem. Soc.* **1983**, *105*, 475.

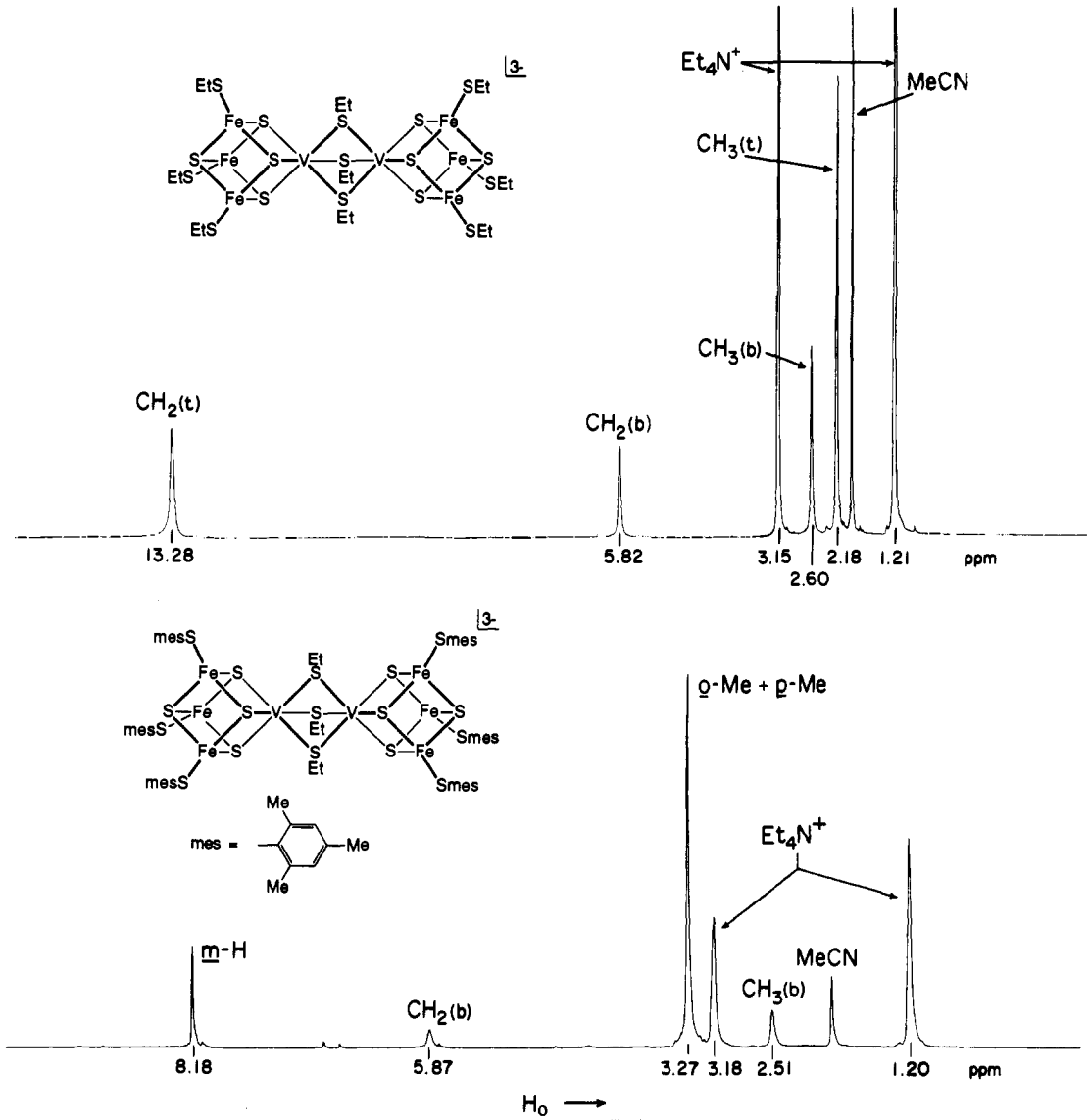

Figure 4. ^1H NMR spectra of $[V_2Fe_6S_8(SEt)_9]^{3-}$ (top) and $[V_2Fe_6S_8(Smes)_6(SEt)_3]^{3-}$ (bottom) in acetonitrile solutions at 295 K; signal assignments are indicated (b = bridging, t = terminal).

clusters with which to examine the influence of changes in heterometal on several key properties: redox potentials, electron distribution in a fixed charge state, and changes in electron distribution attendant to oxidation-reduction. Previous attempts of this sort have been implemented with Fe(II/III)-bridged double cubanes (**5**)[13,17] and diphosphine-ligated single cubanes (**6**) and related single clusters with other terminal ligands at the M site.[2,35] In these cases, property comparisons are less exact because one or more of the constant factors in cluster series **3** was not maintained across more than two or three species. Because of the possibility of relatively small differences in properties, redox potentials and Mössbauer spectra were each measured under identical conditions. In addition, we shall of necessity make use of limited data drawn from earlier work on clusters **5–9**, which are schematically depicted in Figure 5.

Redox Potentials. In previous work, it has been shown that the double cubane clusters **3** with M = Mo and W exhibit two chemically reversible redox steps in the range −1.0 to −2.0 V whose peak potentials in aprotic solvents are separated by the relatively narrow interval of 170–220 mV.[13,17b,36] These reactions define the three-membered electron-transfer series **3**, to which the potentials in Table II correspond. Potentials were determined

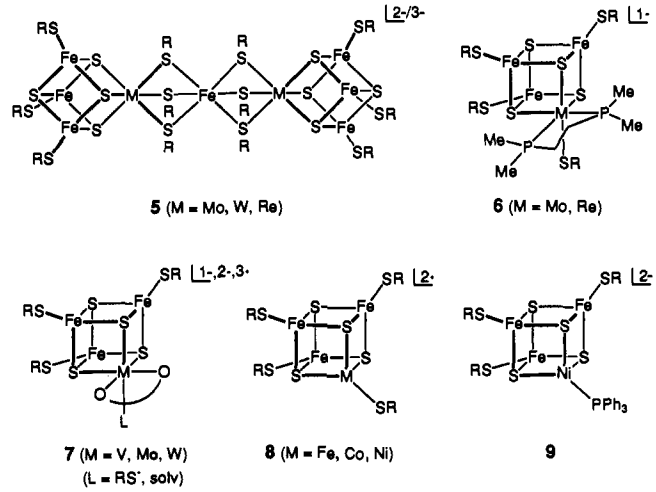

Figure 5. Structural formulas of heterometal cubane-type clusters relevant to the present work, including the Fe(II,III)-bridged double cubanes (**5**) and single cubanes with terminal diphosphine (dmpe, **6**), catecholate (**7**), thiolate (**8**), and triphenylphosphine (**9**) ligands at the heterometal site.

(35) Carney, M. J.; Kovacs, J. A.; Zhang, Y.-P.; Papaefthymiou, G. C.; Spartalian, K.; Frankel, R. B.; Holm, R. H. *Inorg. Chem.* **1987**, *26*, 719.
(36) Christou, G.; Garner, C. D.; Miller, R. M.; Johnson, C. E.; Rush, J. D. *J. Chem. Soc., Dalton Trans.* **1980**, 2363.

$$[M_2Fe_6S_8(SEt)_9]^{3-} \underset{-e^-}{\overset{+e^-}{\rightleftharpoons}} [M_2Fe_6S_8(SEt)_9]^{4-} \underset{-e^-}{\overset{+e^-}{\rightleftharpoons}} [M_2Fe_6S_8(SEt)_9]^{5-} \quad (3)$$

under identical conditions. Rutstrom and Robbat,[37] in a detailed study, have demonstrated the electrochemical reversibility of these processes for the molybdenum clusters. The cyclic and differential pulse voltammograms of $[V_2Fe_6S_8(SEt)_9]^{3-}$ shown in Figure 6 are typical of the clusters in Table II. These values tend to follow expected periodic trends, with potentials decreasing (reductions becoming more difficult) in the order V ≈ Nb < Ta and Mo < W.[38] The Nb < Ta and Mo < W trends also hold in the $[MCl_6]^{-z/-(z+1)}$ series (z = 1, 2) in dichloromethane,[39] but the potential differences in these cases are much greater because of considerably less electron delocalization compared to the clusters. For example, in the Mo/W series with z = 1 and 2, the differences are 0.65 and 0.87 V, respectively, whereas in series 3 the differences are only 0.12 and 0.09 V, respectively.

Correlation of Isomer Shift and Iron Oxidation State. Prior to considering the ^{57}Fe isomer shifts of heterometal clusters, a relationship between shift and iron (mean) oxidation state s is introduced. While we have presented correlations of this type previously,[12,14] isomer shift data of both Fe–S and MFe_3S_4 clusters were employed, and some data had to be corrected for second-order Doppler shifts owing to differences in temperature of the reference. Some isomer shifts were referenced to iron metal at 4.2 K rather than at room temperature, now the convention. In the present work, we have utilized previously unavailable literature results, measured all compounds at 4.2 K, and restricted the correlation to iron–sulfur compounds containing two or three sulfide ligands at the iron sites. Isomer shifts of the four clusters $[Fe_4S_4(S\text{-}t\text{Bu})_4]^{3-}$ ($Fe^{2.25+}$, 0.51 mm/s), $[Fe_4S_4(SEt)_4]^{2-}$ ($Fe^{2.5+}$, 0.44 mm/s), $[Fe_4S_4(S\text{-}2,4,6\text{-}i\text{Pr}_3C_6H_2)_4]^-$ ($Fe^{2.75+}$, 0.37 mm/s[40]), and $[Fe_2S_2(SEt)_4]^{2-}$ (Fe^{3+}, 0.27 mm/s), and of the three oxidation states of the protein-bound Fe_3S_4 clusters, taken from the results of Münck and co-workers[3,9,10b,41] and presented in Figure 7, were employed. Least-squares fit of the data afforded eq 4 (r^2 = 0.991), which pertains to tetrahedral $FeS_{4-n}(SR)_n$ coordination (n = 1, 2) at 4.2 K vs iron metal at room temperature.[42]

$$\delta = 1.36 - 0.36s \quad (4)$$

Charge Distribution. The zero-field Mössbauer spectra of the clusters **3** with M = Mo and W have been reported,[12,14,36] but not necessarily with the same cation nor under uniform conditions of temperature with regard to both absorber and standard. We have determined the spectra of the vanadium, niobium, and rhenium clusters and remeasured other clusters, all as polycrystalline solids at 4.2 K. All spectra consist of an apparent single quadrupole doublet, as illustrated with $(Et_4N)_3[V_2Fe_6S_8(SEt)_9]$ in Figure 8. These were analyzed in terms of one doublet. Within the resolution of the technique at zero applied magnetic field, the iron atoms are equivalent. Isomer shifts (δ) and quadrupole splittings (ΔE_Q) of the Et_4N^+ salts of six double-cubane clusters (boldface) are presented in Table IV together with other data for several clusters of types **5**–**7**.[2,35,43] The results are organized in terms of core oxidation state. For the clusters **3**, the isomer shifts increase in the order M = V < Mo ≈ Nb < W ≈ Re. Note that the *trend in isomer shifts parallels that in redox potentials*; i.e., as the ferrous character of the core increases the redox potentials become more negative. We are unaware of a previous correlation of this type for clusters.

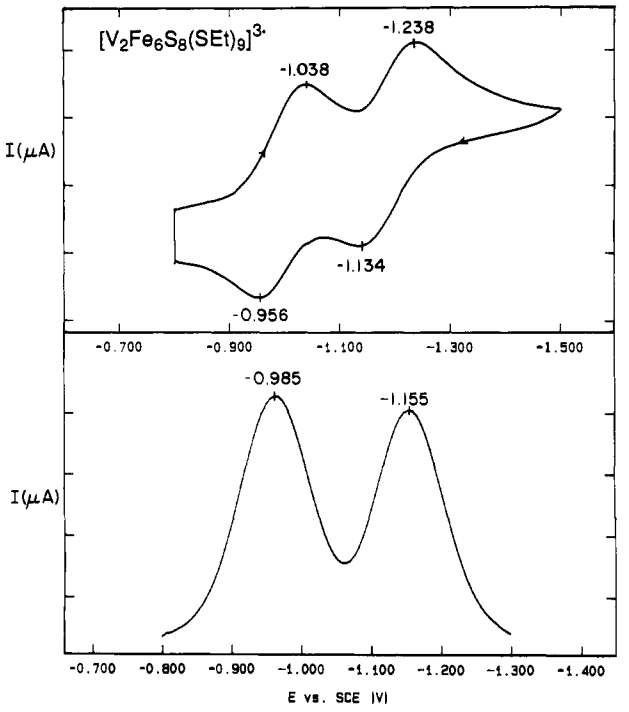

Figure 6. Cyclic voltammogram (top, 100 mV/s) and differential pulse voltammogram (bottom) of $[V_2Fe_6S_8(SEt)_9]^{3-}$ in acetonitrile solution at room temperature; peak potentials vs SCE are indicated.

Changes in Charge Distribution upon Reduction. The isomer shifts of synthetic and protein-bound heterometal cubane clusters are displayed for purposes of comparison in Figure 7. The results include those for double cubanes as well as for other clusters in Table V. The entry $[FeFe_3S_4]^{2+}$ refers to the substite-differentiated species $[FeFe_3S_4(LS_3)(RNC)_3]^-$,[44] in which the unique subsite containing low-spin Fe(II) is a pseudoheteormetal. The isomer shift differences between the adjacent oxidation levels $[VFe_3S_4]^{2+/3+}$, $[NbFe_3S_4]^{2+/3+}$, $[MoFe_3S_4]^{2+/3+}$, and $[CoFe_3S_4]^{+/2+}$ span a narrow range (0.09–0.12 mm/s). Of synthetic species, only the shift of $[VFe_3S_4]^{2+}$ [35] is not taken from a type **3** cluster. The cobalt-containing clusters are protein bound.[8] If in series 3 or related redox reactions, electron density changes are confined to the Fe_3S_4 cluster fragments, $\delta_{ox} - \delta_{red}$ = 0.12 mm/s is estimated from the correlation of eq 4. If the isomer shifts of the protein-bound $[Fe_3S_4]^z$ clusters are taken as internal calibrants, then a difference of 0.14 mm/s is expected. By either approach, it is evident that the redox reactions of heterometal clusters, at least over the oxidation states available, *dominantly affect the charge distribution within the Fe_3S_4 portions of the clusters.*

Spin States. The ground-state spins of nearly all MFe_3S_4 clusters have been determined, either by magnetic susceptibility determinations or spectroscopic analysis. The five states that

(37) Rutstrom, D. J.; Robbat, A., Jr. *J. Electroanal. Chem.* **1986**, *200*, 193.

(38) An earlier report of the potential order W > Mo for the $[M_2Fe_6S_8(SEt)_9]^{3-/4-}$ couple in Me_2SO solution[36] does not conform with the expected trend, which is also followed by the $[M_2Fe_6Se_8(SEt)_9]^{-z/-(z+1)}$ couples (z = 3, 4) in acetonitrile.[18]

(39) Heath, G. A.; Moock, K. A.; Sharp, D. W. A.; Yellowless, L. J. *J. Chem. Soc., Chem. Commun.* **1985**, 1503.

(40) Papaefthymiou, V.; Millar M. M.; Münck, E. *Inorg. Chem.* **1987**, *25*, 3010.

(41) (a) Emptage, M. H.; Kent, T. A.; Huynh, B. H.; Rawlings, J.; Orme-Johnson, W. H.; Münck, E. *J. Biol. Chem.* **1980**, *255*, 1793. (b) Huynh, B. H.; Moura, J. J. G.; Moura, I.; Kent, T. A.; LeGall, J.; Xavier, A.; Münck, E. *J. Biol. Chem.* **1980**, *255*, 3242. (c) Kent, T. A.; Dreyer, J.-L.; Kennedy, M. C.; Huynh, B. H.; Emptage, M. H.; Beinert, H.; Münck, E. *Proc. Natl. Acad. Sci. U.S.A.* **1982**, *79*, 1096. (d) Surerus, K. K.; Kennedy, M. C.; Beinert, H.; Münck, E. *Proc. Natl. Acad. Sci. U.S.A.* **1989**, *86*, 9846.

(42) Although this fit has somewhat more scatter than that which does not include the shifts of Fe_3S_4 clusters (δ = 1.23 – 0.32s, r^2 = 0.997), it is more effective in correlating a wider data set. $[Fe(SEt)_4]^{2-}$ does not fit well; $[Fe(SEt)_4]^-$ fits both correlations but has not been included because it lacks sulfide ligands.

(43) Mascharak, P. K.; Papaefthymiou, G. C.; Armstrong, W. H.; Foner, S.; Frankel, R. B. *Inorg. Chem.* **1983**, *22*, 2851.

(44) Weigel, J. A.; Srivastava, K. K. P.; Day, E. P.; Münck, E.; Holm, R. H. *J. Am. Chem. Soc.* **1990**, *112*, 8015.

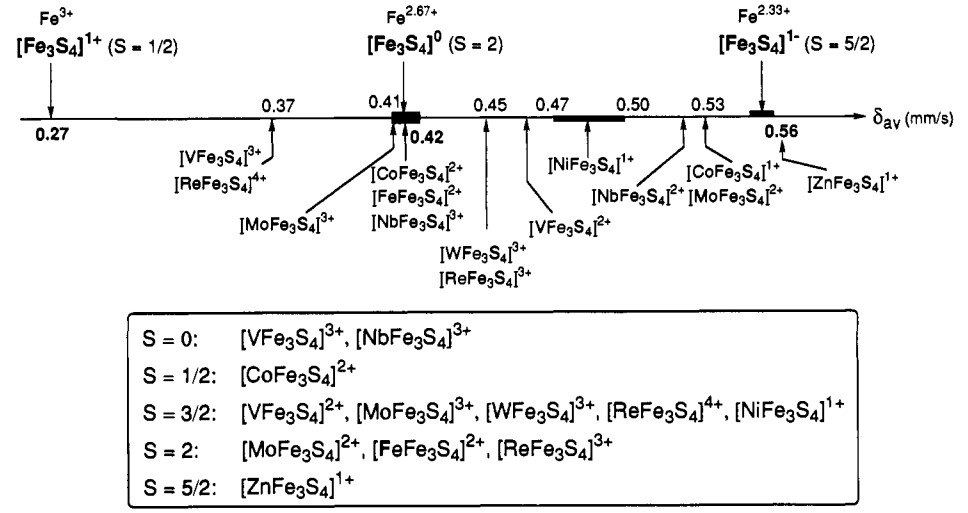

Figure 7. Comparison of the (mean) isomer shifts of $[Fe_3S_4]^z$ and $[MFe_3S_4]^z$ clusters with M = V, Nb, Mo, W, Re, Co, Ni, and Zn. For a given $[MFe_3S_4]^z$ cluster, the shifts refer to the double cubanes **3** if available. Otherwise, shifts are taken from additional data in Table V, protein-bound clusters,[8,9,10b] and elsewhere.[44] Bars indicate the range of values for a given oxidation state. Spin states of cluster cores are indicated.

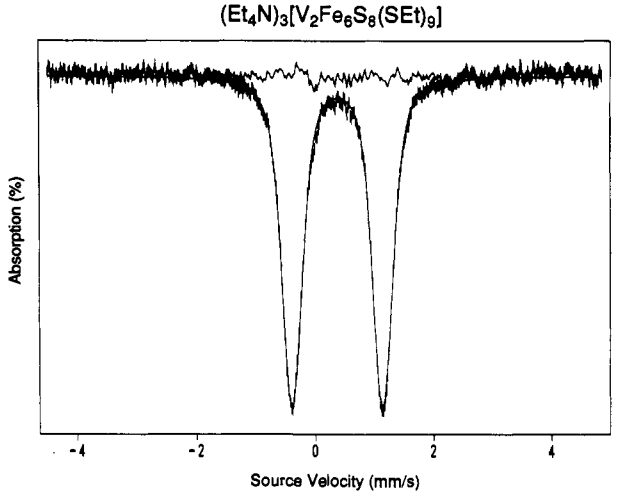

Figure 8. The zero-field Mössbauer spectrum of polycrystalline $(Et_4N)_3[V_2Fe_6S_8(SEt)_9]$ recorded at 4.2 K.

have been detected are summarized in Figure 7; specific examples are given in Table V. There is no known case in which the spin state of a given core is dependent on ligation. All clusters exhibit isotropically shifted ^1H NMR spectra which are usually very well resolved and whose isotropic shift patterns of ligands at iron sites are consistent with dominant contact interactions. Spectra which bear out this behavior have been given elsewhere.[45] Among the new clusters, the spectrum of $[V_2Fe_6S_8(SEt)_9]^{3-}$ (Figure 4) illustrates these points. The negative isotropic shift of the terminal methylene protons arises from ligand → metal antiparallel spin delocalization. Treatment of type **3** clusters with arenethiols results in terminal but not bridging ligand substitution.[30b] Thus, reaction 5 with mesitylthiol proceeds to completion with a slight excess of thiol. The spectrum of the product (Figure 4) reveals

$$[V_2Fe_6S_8(SEt)_9]^{3-} + 6mesSH \rightarrow [V_2Fe_6S_8(SEt)_3(Smes)_6]^{3-} + 6EtSH \quad (5)$$

negative isotropic shifts of *o*-Me, *p*-Me, and *m*-H, as required for contact interactions by antiparallel spin.[46] The behavior of

Table IV. Mössbauer Spectroscopic Parameters of $(Et_4N)_3[M_2Fe_6S_8(SEt)_9]$ and Related $[MFe_3S_4]^z$ Clusters

core	cluster	mm/s δ_{av}[a]	mm/s ΔE_Q[b]	ref
$[VFe_3S_4]^{3+}$	$[V_2Fe_6S_8(SEt)_9]^{3-}$ (**3**)	**0.37**	1.54	*c*
$[VFe_3S_4]^{2+}$	$[VFe_3S_4(SR)_3(DMF)_3]^{-}$ [d]	0.46		35
$[NbFe_3S_4]^{3+}$	$[Nb_2Fe_6S_8(SEt)_9]^{3-}$ (**3**)	**0.42**	1.83	*c*
$[NbFe_3S_4]^{2+}$	$[Nb_2Fe_6S_8(SEt)_9]^{5-}$ (**3**)	**0.52**	1.62	*c*
$[MoFe_3S_4]^{3+}$	$[Mo_2Fe_6S_8(SEt)_9]^{3-}$ (**3**)	**0.41**	1.03	*c*
	$[Mo_2Fe_6S_8(SPh)_9]^{3-}$ (**3**)	0.42		14
	$[Mo_2Fe_7S_8(SEt)_{12}]^{3-}$ (**5**)	0.42		13
	$[MoFe_3S_4(SR)_4(al_2cat)]^{2-}$ [e,f]	0.42		43
	$[MoFe_3S_4(SEt)_4(dmpe)]^{-}$ [g] (**6**)	0.41		35
$[MoFe_3S_4]^{2+}$	$[Mo_2Fe_6S_8(SPh)_9]^{5-}$ (**3**)	0.53		14
	$[MoFe_3S_4(SR)_3(al_2cat)(EtCN)]^{3-}$ [e] (**7**)	0.53		43
$[WFe_3S_4]^{3+}$	$[W_2Fe_6S_8(SEt)_9]^{3-}$ (**3**)	**0.45**	1.38	*c*
	$[W_2Fe_6S_8(\mu_2\text{-}OMe)_3(SPh)_6]^{3-}$	0.47		36
	$[W_2Fe_7S_8(SEt)_{12}]^{3-}$ (**5**)	0.43		13
$[ReFe_3S_4]^{4+}$	$[Re_2Fe_7S_8(SEt)_{12}]^{2-}$ (**5**)	0.37		17a
$[ReFe_3S_4]^{3+}$	$[Re_2Fe_6S_8(SEt)_9]^{3-}$ (**3**)	**0.45**	1.01	*c*
	$[ReFe_3S_4(SEt)_4(dmpe)]^{-}$ (**6**)	0.48		2

[a] ±0.01 mm/s. [b] Values omitted are not relevant to present arguments and may be found in the references. [c] This work. [d] R = *p*-C_6H_4Me. [e] R = *p*-C_6H_4Cl. [f] al_2cat = 3,6-diallylcatecholate(2–). [g] dmpe = 1,2-dimethylphosphinoethane.

$[Nb_2Fe_6S_8(SEt)_9]^{3-}$ is entirely similar. However, the isotropic shifts of these species are considerably smaller than those of other heterometal cubane clusters (Table V). Magnetic measurements of polycrystalline $(Et_4N)_3[V_2Fe_6S_8(SEt)_9]$ revealed that the cluster has an $S = 0$ ground state and that above *ca.* 100 K paramagnetic excited state(s) are populated such that at 300 K $\mu_{eff} = 1.85\ \mu_B$. This behavior is very similar to that of $[Fe_4S_4]^{2+}$ clusters, which also have a diamagnetic ground state and populate low-lying excited state(s) with $S > 0$.[47] Presumably, in the same way, $[M_2Fe_6S_8(SEt)_9]^{3-}$ (M = V, Nb) clusters develop isotropic shifts that are comparable to those of $[Fe_4S_4]^{2+}$ clusters.

Because contact shifts can be approximated as proportional to magnetic susceptibility,[48] we have examined the relationship between spin state and isotropic shifts of iron–thiolate ligands for a variety of MFe_3S_4 clusters. We have chosen to use the methylene shifts of ethanethiolate because of their large values, and the *m*-H shifts of benzenethiolate or, where possible for the sake of uniformity, mesitylthiolate. The latter are relatively small but

(45) For presentation of spectra and discussion, *cf* refs 2, 13, 14, 16, 17b, 30b, 33, 34, and 44.

(46) La Mar, G. N. In *NMR of Paramagnetic Molecules*; La Mar, G. N., Horrocks, W. D., Holm, R. H., Eds.; Academic Press: New York, 1973; Chapter 3.

(47) Laskowski, E. J.; Frankel, R. B.; Gillum, W. O.; Papaefthymiou, G. C.; Renaud, J.; Ibers, J. A.; Holm, R. H. *J. Am. Chem. Soc.* **1978**, *100*, 5322.

(48) For theoretical treatments, *cf.*: (a) Bertini, I.; Luchinat, C. *NMR of Paramagnetic Molecules in Biological Systems*; Benjamin/Cummings, Inc.: Menlo Park, CA, 1986; Chapters 2 and 7. (b) Banci, L.; Bertini, I.; Luchinat, C. *Struct. Bonding (Berlin)* **1990**, *72*, 113.

Table V. ^{1}H NMR Isotropic Shifts as Spin State Indicators (CD_3CN Solutions, 293–299 K)

cluster	S	$(\Delta H/H_0)_{iso}$,[a] ppm SCH_2[b]	ppm m-H[c]	ref
$[Fe_4S_4(SR)_4]^{2-}$ (8)	0	−10.2	−1.43	d
$[V_2Fe_6S_8(SEt)_3(SR)_6]^{3-}$ (3)	0	−10.8	−1.57	d
$[Nb_2Fe_6S_8(SEt)_3(SR)_6]^{3-}$ (3)	0	−14.0	−1.98	d
$[CoFe_3S_4(Smes)_4]^{2-}$ (8)	1/2		−3.97	5
$[NiFe_3S_4(SR)_4]^{3-}$ (8)	3/2	−53.2	−6.88	4, 5
$[NiFe_3S_4(PPh_3)(SR)_3]^{2-}$ (9)	3/2	−55.7	−6.94	4, 5
$[Mo_2Fe_6S_8(SEt)_3(SR)_6]^{3-}$ (3)	3/2	−53.2	−7.02	13, d
$[MoFe_3S_4(SR)_3(al_2cat)(solv)]^{2-}$ [e] (7)	3/2	−47.6	−6.50[f]	33
$[W_2Fe_6S_8(SEt)_3(SR)_6]^{3-}$ (3)	3/2	−51.8	−7.06	16, d
$[WFe_3S_4(SR)_3(al_2cat)(solv)]^{2-}$ (7)	3/2	−42.2	−6.29[f]	33
$[Mo_2Fe_6S_8(SPh)_9]^{5-}$ (3)	2		−8.86	14
$[MoFe_3S_4(SR)_3(al_2cat)(MeCN)]^{3-}$ [g] (7)	2		−9.40	34
$[WFe_3S_4(SR)_3(al_2cat)(MeCN)]^{3-}$ [g] (7)	2		−9.30	34
$[Re_2Fe_6S_8(SEt)_3(SR)_6]^{3-}$ (3)	2	−58.7	−9.05	2, 17b, d

[a] $(\Delta H/H_0)_{iso} = (\Delta H/H_0)_{dia} - (\Delta H/H_0)_{obs}$; diamagnetic references are EtSH and $(Et_4N)(SAr)$. [b] R = Et. [c] R = mesityl unless otherwise indicated. [d] This work. [e] al_2cat = 3,6-diallylcatecholate(2–). [f] R = Ph in DMSO. [g] R = p-C_6H_4Cl.

the signals are always sharp and more clusters have been prepared with these ligands. The results, presented in Table V, show a definite relationship between shift and spin state. For m-H shifts, the following ranges (ppm) are apparent: $S = 0$, −1.4 to −2.0; $S = {}^1/_2$, −4.0 (one example); $S = {}^3/_2$, −6.3 to −7.1; $S = 2$, −8.8 to −9.4. These non-overlapping ranges imply a Curie-type susceptibility in solution, with little or no population of excited states that would significantly influence the strength of the contact interactions for $S > 0$.[49] Under these circumstances, isotropic shifts at *ca.* 300 K are meaningful indicators of cluster spin states.

$[Fe_3S_4]^z$ as a Ligand. The ligand function of this cuboidal entity has been demonstrated by the formation of $[MFe_3S_4]^z$ clusters from protein-bound $[Fe_3S_4]^{0,-}$ and exogenous metal ions.[3,8-11] Inasmuch as the cuboidal cluster has never been isolated as a stable entity outside of a protein matrix,[50] this function has not yet been demonstrated in synthetic systems. However, the cluster is a *conceptual* ligand in the variety of synthetic $[MFe_3S_4]^z$ clusters obtained in self-assembly systems or by reductive rearrangement reactions.[3] The question then arises as to the zeroth order description of charge over the Fe_3S_4 and M portions of the cluster core and the innocence, or lack thereof, of the cluster ligand. We examine these matters with reference to the isomer shift plot in Figure 7. A number of species fall within ±0.02 mm/s of $[Fe_3S_4]^0$ or $[Fe_3S_4]^-$, this margin also being a reasonable estimate of the errors in isomer shifts from different sources. In these cases, the cluster ligand oxidation state, and by difference that of M, would appear to be described. We have observed elsewhere that this approach allows a rationalization of cluster spins.[3,5] For clusters with tetrahedral M sites, antiparallel coupling of the M^{2+} spin with that of $[Fe_3S_4]^{0/-}$ yields the observed spin. (For $[NiFe_3S_4]^+$, this requires $[Fe_3S_4]^-$ as the ligand, despite the intermediate value of the isomer shift.) For six-coordinate metal sites, a similar coupling scheme involving trigonally distorted M, with the energy order $e < a_1$ for orbitals of t_{2g} parentage in $d^{3,4}$ cases, affords the observed spin.

Cluster species whose isomer shifts do not correlate relatively closely with cluster ligands are $[VFe_3S_4]^{2+,3+}$ and $[ReFe_3S_4]^{4+}$, and $[NiFe_3S_4]^+$. The spins of the latter two species can be rationalized in terms of the ligands $[Fe_3S_4]^0$ and $[Fe_3S_4]^-$, respectively. However, the same scheme does not account for the $S = 0$ state of $[VFe_3S_4]^{3+}$ and $[NbFe_3S_4]^{3+}$, despite the fact that the isomer shift of the latter accords exactly with that of $[Fe_3S_4]^0$. It should be noted that the shifts of both oxidation states of the vanadium-containing clusters depart considerably from those of $[Fe_3S_4]^{0,-}$.[51] At present, we have no satisfactory explanation of the diamagnetic ground state of these clusters. Clearly, a detailed spin coupling model must be developed for $[MFe_3S_4]^z$ clusters.

Summary. The following are the principal results and conclusions of this investigation.

1. The cluster assembly method affords the new heterometal double-cubane clusters $[V_2Fe_6S_8(SEt)_9]^{3-}$ (71%), $[Nb_2Fe_6S_8(SEt)_9]^{3-}$ (33%), and $[Nb_2Fe_6S_8(SEt)_9]^{5-}$ (12%) as their Et_4N^+ salts in the indicated yields.

2. The trianionic clusters in (1), together with those prepared previously, form a set of five clusters $[M_2Fe_6S_8(SEt)_9]^{3-}$ (M = V, Nb, Mo, W, Re) that are structurally congruent and virtually isodimensional; their Et_4N^+ salts are isomorphous. These properties facilitate elucidation of property differences owing to variation in heterometal at parity of cluster composition and structure.

3. Redox potentials for the 3–/4– and 4–/5– conversions decrease in the order V > Nb > Ta > Mo > W > Re and qualitatively correlate with the order of increasing isomer shift V (0.37 mm/s) < Nb ≈ Mo < W ≈ Re (0.45 mm/s); reductions become more difficult as the ferrous character of the core atoms increases.

4. On the basis of a correlation between oxidation state and isomer shift for Fe–S clusters, shift differences between the core oxidation states $[MFe_3S_4]^{2+/3+}$ (M = V, Nb, Mo) and $[CoFe_3S_4]^{+/2+}$ (0.09–0.12 mm/s) correspond to charge distribution changes mainly affecting the Fe_3S_4 cluster portions.

5. The cuboidal $[Fe_3S_4]^{0,-}$ cluster cores have a demonstrable ligand function in the formation of protein-bound heterometal clusters $[MFe_3S_4]^z$ and are, at the least, conceptual ligands in clusters prepared by self-assembly or reductive rearrangement. Oxidation state designations of the cluster ligand and M atoms follow reasonably from comparison of isomer shifts with those of $[Fe_3S_4]^{0,-}$ for most clusters. Cluster spins can be rationalized by a simple scheme but the diamagnetism of $[MFe_3S_4]^{3+}$ (M = V, Nb) cannot be explained in this way.

6. The ambient temperature isotropic shifts of methylene and m-H protons of ethanethiolate and phenylthiolate ligands, respectively, at Fe sites serve as convenient indicators of the ground spin state of $[MFe_3S_4]^z$ clusters.

Relation to the Cofactor Clusters of Nitrogenase. The highly similar coordination environments of molybdenum and vanadium atoms in the cofactors and in $MoFe_3S_4$ and VFe_3S_4 clusters, respectively, have been established by EXAFS.[3,22,52] This strongly indicates that these two atoms occupy corresponding stereochemical positions in their cofactors, which possibly (if not probably) have the same core structure as **4**. If so, the results of this work signify the likely influence of heterometal on those cluster properties that derive in substantial part from the MFe_3S_3 portion of the cofactor. These include appreciable differences in redox potentials linking isoelectronic states, modulation of electron distribution at iron sites, and localization of principal charge density changes attendant to redox reactions at those sites. In the clusters **3** (M = V, Mo), these effects are appreciable. There is a 270–280-mV difference in redox potentials for two successive reactions involving clusters with the same charge (Table II). For

(49) Unless there are significant dipolar contributions,[48] the *ca.* 30% larger isotropic shifts for $[Nb_2Fe_6S_8(SEt)_9]^{3-}$ than $[V_2Fe_6S_8(SEt)_9]^{3-}$ arise from differences in populations of excited states.

(50) Roth, E. K. H.; Jordanov, J. *Inorg. Chem.* **1992**, *31*, 240.

(51) The scheme affords the $S = {}^3/_2$ state of $[VFe_3S_4]^{2+}$ clusters by antiparallel coupling of V^{2+} (e^3 or $a_1{}^2e^1$, $S = {}^1/_2$) with $[Fe_3S_4]^0$ ($S = 2$). The $S = 0$ state of $[VFe_3S_4]^{3+}$ follows from similar coupling of V^{2+} with $[Fe_3S_4]^+$ ($S = {}^1/_2$) but this is not consistent with the isomer shift scale (Figure 7).

(52) (a) Conradson, S. D.; Burgess, B. K.; Newton, W. E.; Mortenson, L. E.; Hodgson, K. O. *J. Am. Chem. Soc.* **1987**, *109*, 7507. (b) Arber, J. M.; Dobson, B. R.; Eady, R. R.; Stevens, P.; Hasnain, S. S.; Garner, C. D.; Smith, B. E. *Nature* **1987**, *325*, 372. (c) Arber, J. M.; Dobson, B. R.; Eady, R. R.; Hasnain, S. S.; Garner, C. D.; Matsushita, T.; Nomura, M.; Smith, B. E. *Biochem. J.* **1989**, *258*, 733. (d) George, G. N.; Coyle, C. L.; Hales, B. J.; Cramer, S. P. *J. Am. Chem. Soc.* **1988**, *110*, 4057.

the isoelectronic cluster cores $[VFe_3S_4]^{2+}/[MoFe_3S_4]^{3+}$, the isomer shift difference is 0.04–0.05 mm/s, and for cluster cores of equal charge, the shift differences are 0.07 mm/s (2+) and 0.04–0.05 mm/s (3+) (Table IV). In each comparison, the vanadium-containing cluster sustains the more reduced Fe_3S_4 fragment, a property which, as already observed, is consistent with the order of redox potentials. The large difference in potentials for reactions in which electron density changes largely occur in Fe_3S_4 cluster portions emphasizes the role of the heterometal in stabilizing core oxidation levels.

Acknowledgment. This research was supported by NIH Grant GM 28856. X-ray diffraction equipment was obtained by NIH Grant 1 S10 RR 02247.

Supplementary Material Available: Tables of crystallographic data for $(Et_4N)_3[V_2Fe_6S_8(SEt)_9]$, including intensity collection, positional and thermal parameters, and interatomic distances and angles (5 pages); listing of calculated and observed structure factors (13 pages). Ordering information is given on any current masthead page.